CHAPTER TWO

SOURCE PROCESSES AND SEISMIC SOURCES ON STROMBOLI

2.1 Introduction

It is generally believed that the eruptive style of Stromboli over the past few millenia has been very similar to that observed even today. Typically there are several eruptive events per hour in which high-pressure gas bursts from a vent, driving clots of lava up to 200 m above the vents, which then trace ballistic trajectories and are cool upon landing. Strombolian eruptions are generally attributed to the bursting of bubbles at the air/magma surface.

Luckett [1997] concluded that the source of the very-long-period (VLP) signals recorded at Stromboli in 1995 is 600-700 m below the vents, which suggests that although these phases coincide with eruptions, they are not caused by bubble burst. Based on 1995 data, *Forbriger and Wielandt* [1997] placed the VLP source much shallower - 135 m below the vents - but even this is too deep to correspond to bursting bubbles. This highlights two important problems related to these VLP phases: (1) Why are these estimates of source depth so different? (2) What processes lead to the generation of VLP phases?

Stromboli has been studied extensively in the last 10 years using many geophysical techniques [e.g. *Falsaperla and Schick,* 1993] and in this chapter some of the results are summarised. The emphasis is on constraining the location of seismic sources and the geometry of the magmatic system, since these parameters are important for modelling. There is also a discussion of volcanic processes, in order to determine which of these have the potential to generate large pressure changes, and thereby act as significant sources of seismicity.

An overview of this chapter is presented in Section 1.5.

2.2 Stromboli background

2.2.1 Geological context

Stromboli (38.789°N, 15.213°E) is the northeastern most and youngest member of the Aoelian islands, a volcanic arc which lies off the north coast of Sicily [Fig. 2.1], resulting from the subduction of the African plate beneath the Eurasian plate. Stromboli is a strato-volcano rising 3 km from the Tyrrhenian sea floor, comparable in size to Etna. The submarine volume of Stromboli is 230 km^3, whilst only 4 km^3 (the upper 924 m) protrudes above sea level [*Allard* et al., 1994] forming an island roughly 4.5 km by 3.5 km. The average slope is 13° at the base, increasing upwards.

The highest point of the volcano, Serra di Vancori, lies to the south-west at 924 m above sea-level and represents the southern rim of an ancient crater. The active craters however are situated on the north-west side about 700 m above sea-level, and below another peak, the Pizzo sopra la Fossa. This has a mean height of 850 m above sea-level though its summit reaches 918 m elevation, and is also the remnant of an ancient crater [*Chouet et al*., 1974]. Climbing to this peak takes less than 2 hours and gives a spectacular view of the active vents.

The crateric plain lies at the upper end of a large talus scree which partly fills the depression formed by the collapse of a portion of the volcanic edifice maybe no more than several millenia ago. This talus has a slope of 35°, extends from near the summit to the sea and partially fills a large sector graben, the Sciara del Fuoco [*Giberti et al*., 1992]. Several vents, surrounded by little cones formed by superposition of the erupted materials, are formed on the plain. Presently there are three craters aligned in a roughly NE-SW direction.

The Sciara del Fuoco is bounded by two conspicuous cliffs, to the northeast (Filo del Fuoco) and south (Filo di Baraona). Both form immense natural barriers protecting the outer slopes of the volcano (beyond the Sciara depression) from lava flows and smaller pyroclastic flows as well as avalanches of material ejected from the craters. [*Simkin and Siebert*, 1994].

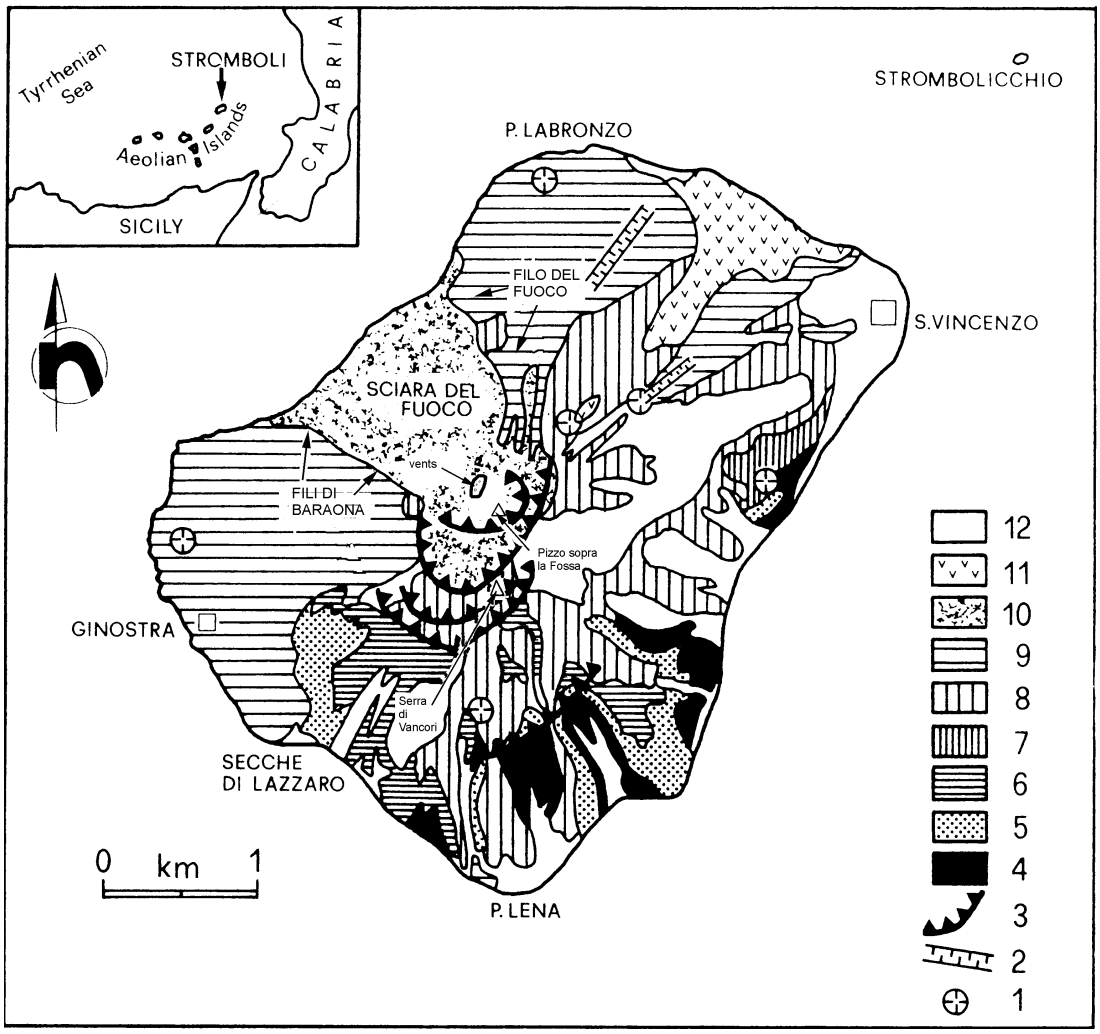

Figure 2.1: Simplified map of Stromboli after *Hornig-Kjarsgaard et al.* [1993]. Key: 1 secondary and eccentric vents; 2 eruptive fissures; 3 crater rim; 4 Paleostromboli I (100000-64000 years ago); 5 Paleostromboli II (64000-55000 years ago); 6 Paleostromboli III (55000-35000 years ago); 7 Sciara complex (35000 years ago); 8 Vancori (25000-13000 years ago); 9 Neostromboli (13000-5000 years ago); 10 recent Strombolian ejecta and subordinate lava flows (<5000 years old); 11 San Bartolo lava flows (<5000 years old); 12 epiclastic and reworked material.

2.2.2 Historic activity

Stromboli is one of the few volcanoes on earth displaying continuous eruptive activity over a period longer than a few years or decades. Descriptions of activity at Stromboli throughout historical time suggest the activity has been unchanged for at least 2500 years. Most of the present cone was well developed 15,000 years ago [*Giberti et al*., 1992].

Normal activity consists of small, discrete explosions during which well-collimated jets of incandescent gases project molten lava fragments to heights of up to 200 m above the vents in eruptions lasting a few seconds [*Chouet et al*., 1974]. These eruptions are usually accompanied by white clouds of steam containing small quantities of ash and typically occur several times per hour. Roar and rush sounds are characteristic of normal degassing, suggesting the outlet of gas under pressure. These sounds are followed by a puff of gas and, occasionally, ejection of pyroclasts. There is little or no effusion of lava [*Blackburn et al*., 1976]. Several explosions occur each hour, which makes Stromboli an excellent target for volcanic studies. When this type of eruption is observed at other volcanoes it is often referred to as a Strombolian eruption.

Occasionally, there are periods of stronger, more continuous activity, with fountaining lasting several hours, violent ejection of blocks and large bombs, and, still more rarely, lava outflow. There have been two large eruptions in this century (in 1919 and 1930) that caused significant damage and killed people who were not in the immediate vicinity of the craters. Such temporary, violent episodes of activity could be the result of great amounts of sea water entering through fractures in the submarine part of the volcano and mixing with magma [*Chouet et al*., 1974; *Giberti et al*., 1992; *Simkin and Siebert*, 1994].

2.2.3 Activity during the 1992 and 1995 experiments

During the period when seismic data was being collected in 1992, Stromboli was constantly active, with eruptions occuring once every ten minutes on average. Between 1992 and 1996 three main vents were active. These are referred to as vents 1, 2 and 3, by *Neuberg et al*. [1994], numbered from south-west to north-east (other authors number them differently). Each of the vents had characteristic eruptive behaviour:

- Eruptions from vent 1 were the loudest and characterised by fierce jets of gas and a broad lava fountain lasting 10-15 s [*Luckett*, 1997]. An ash cloud was often generated, suggesting the failure of a cap rock in response to rising pressure in the conduit. The ash cloud sometimes evolved into a plume [*Neuberg and Luckett*, 1996]. This is similar to low amplitude Vulcanian activity.

- Eruptions at vent 2 were least frequent and characterised by strong gas jets [*Neuberg et al*., 1994] and a sound like a jet engine in an exhalation lasting up to 20 s. Few pyroclasts or lava were observed [*Luckett*, 1997].

- Eruptions at vent 3 were characterised by short (<5 s) violent eruptions generating narrow lava fountains up to 200 m high. Bubbles with diameters of up to 1 m have been observed at this vent [*Vergniolle & Brandeis,* 1994]. Between eruptions continuous bubbling and flaring (due to gas burning) were observed, with small amounts of pyroclasts ejected at low speed [*Luckett*, 1997].

There is no correlation between eruptions at one vent and any other, nor was a correlation found between eruption sizes and repose times [*Luckett*, 1997].

2.3 Seismicity

2.3.1 Acquisition of Leeds broadband seismic data

The seismic data used in this study come from a broadband array deployed on Stromboli in November/December 1992 and a further experiment in July 1995. Nine Guralp CGM-3 three-component broadband seismometers were deployed in an array during the 1992 experiment on the eastern flank of Stromboli [Fig. 2.2]. Five broadband seismometers were deployed in the 1995 experiment; four in a ring around the crater region, and at one of the sites of the 1992 array for cross-checking purposes [Fig. 2.3]. In both experiments video recordings of the crater region were made so that visual activity and seismic activity could be correlated, and seismic data were recorded by Lennartz Mars dataloggers on magneto-optical disks. A sampling frequency of 62.5 Hz was used. Data were prefiltered at a high cut frequency of 25 Hz to prevent aliasing.

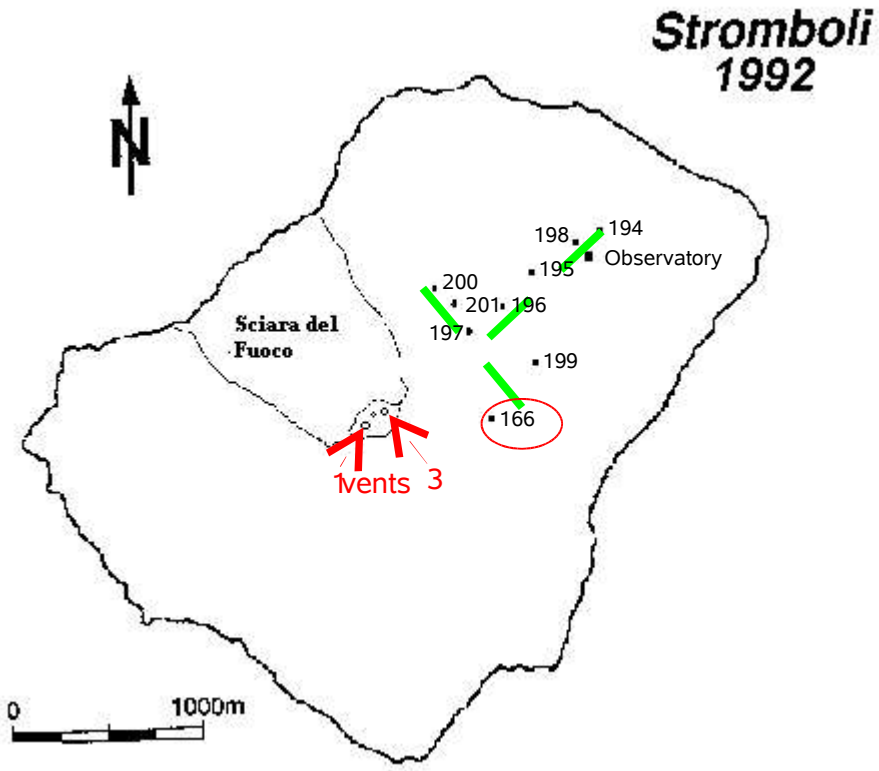

Figure 2.2: Outline map of Stromboli showing the positions of the nine broadband stations deployed in the 1992 experiment. The array forms a T-shape, with the nearest station about 800 m from the vents. For a source directly beneath the craters, this array is incapable of constraining the source location accurately.

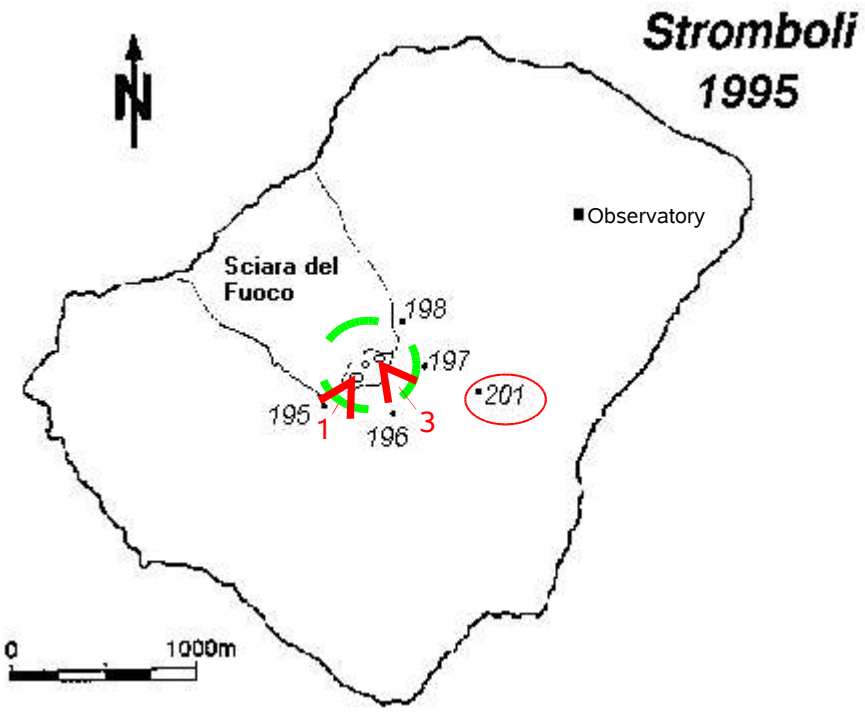

Figure 2.3: Outline map of Stromboli showing the positions of the five broadband stations deployed in the 1995 experiment. Station 201 is identical to station 166 in the 1992 experiment, allowing a direct comparison between the two datasets. The other four stations were deployed in a ring around the vents giving good azimuthal coverage of the crater area, though source depth is poorly constrained.

Huddle tests were performed, prior to deployment of the instruments in the field, to ensure that the seismometers were working correctly and recording the same waveforms.

Seismometers were levelled, oriented to north, protected from rain and buried in pits to a depth of approximately 1 m. Timing information was provided by GPS receivers.

2.3.2 Reconstitution

Raw seismogram

Before the seismic data could be examined they had to be reconstituted. This is the process whereby the original raw seismic data are converted into ground displacement [Fig. 2.4].

The raw seismogram *s(t)* is the convolution of ground velocity *v(t)* with the transfer function of the seismometer *T(t)*. In the frequency domain this is just multiplication:

$$s(\omega) = v(\omega)T(\omega) \qquad \textbf{(2-1)}$$

Transfer function

The transfer function, $T(\omega)$, describes how the seismometer responds to signals of different frequencies. Ideally the transfer function would be flat, meaning the seismometer responds equally at all frequencies, but in reality this can only be partially achieved. Short-period seismometers generally have a flat response down to about 1 Hz. The broadband seismometers used in the 1992 experiment had a flat response down to 0.033 Hz (30 s period), but were modified prior to the 1995 deployment so that they had a flat response down to 0.0083 Hz (120 s period).

A convenient way to describe the transfer function is by poles and zeros. The transfer function for a Guralp seismometer has two low-frequency poles within the unit circle (p_1 and p_2), and two zeroes at the origin of z-plane, and is given by:

$$T(\omega) = \frac{(i\omega)^2}{(i\omega - p_1)(i\omega - p_2)} \qquad \textbf{(2-2)}$$

These poles form a conjugate pair. If they did not, the seismometer would distort the phase of the incoming signal, which is undesirable.

Figure 2.4

Reconstitution step 1: Deconvolution

Ground velocity is recovered by deconvolving the transfer function from the raw seismic trace, which is division in the frequency domain:

$$v(\omega) = \frac{s(\omega)}{T(\omega)} \quad \textbf{(2-3)}$$

Before deconvolution is performed, three steps are necessary:

1. When a Fourier transform of the signal is taken, the signal is assumed to be periodic. It is therefore necessary to remove the linear trend or the Fourier transform will include spectral peaks associated with a sawtooth function. Similarly the offset (mean) must be removed else the Fourier transform may include spectral peaks associated with a square wave function, in addition to a spectral peak at 0 Hz.

2. The data should be **tapered** which forces the signal to zero at both ends. This reduces ringing, which is an undesirable effect of filtering.

3. A **high-pass-filter** must be applied before deconvolution, or low frequency noise magnified by deconvolution might mask the signal. If a lower value for the high-pass frequency is chosen, the reconstituted signal will generally be larger and simpler in shape [Fig. 2.5].

The signal of interest should be padded on both ends to prevent the taper diminishing the amplitude of the signal. For example, if a 30% taper is applied, then the signal of interest should be padded so that it occupies the middle 40% of the reconstituted data.

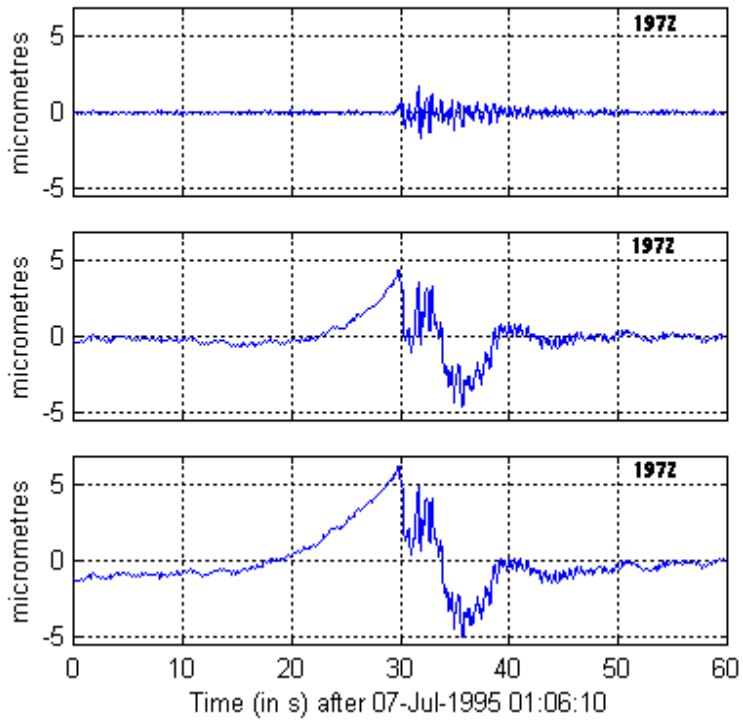

Figure 2.5: Seismogram corresponding to an eruption at vent 1 reconstituted to 3 different periods: (top) 1 s, (middle) 30 s, (bottom) 500 s. Scale is the same for each trace. Top trace corresponds to what would be recorded on a short-period seismometer. Middle trace shows that very-long period phases are dominant. Bottom trace shows that there is even some signal between 30 s and 500 s. Sampling frequency is 31.25 Hz. Data is from vertical component of station 197.

Reconstitution step 2: Integration

Seismic displacement, *x(t)*, is easier to interpret than velocity, so integration is the next step in the reconstitution process. Integration in the time domain is equivalent to division by $i\omega$ in the frequency domain:

$$x(\omega) = v(\omega)\frac{1}{i\omega} \qquad \textbf{(2-4)}$$

2.3.3 Signal types

There are broadly two types of signals commonly observed at Stromboli: eruption related signals and continuous signals (volcanic tremor). The eruption related signals have themselves been further subdivided according to the frequency content of the signal. Reconstituting the signal down to 1 Hz (using a high-pass filter with a 1 Hz corner frequency) shows short-period (SP) eruption phases. Reconstituting the signal down to 100 s shows very-long-period (VLP) phases which are much larger, and have a simpler waveform, than the corresponding short-period (SP) phases. Analysis of huddle test data recorded at Stromboli should reveal whether signals recorded at 1000 s are coherent, and therefore possibly due to magma migration, or just amplified noise.

Volcanic tremor [*Ntepe and Dorel*, 1990; *Del Pezzo et al*., 1992; *Ripepe et al.*, 1993] which typically peaks in the 1-3 Hz band, and SP signals [e.g. *Braun and Ripepe*, 1993; *Ripepe et al.,* 1996; *Ereditato and Luongo*, 1997] have been studied extensively, since these are the only signals which show up on standard short-period (> 1 Hz) seismometers. VLP signals [e.g. *Neuberg et al*., 1994; *Luckett,* 1997] have only been recorded in this decade, because prior to this broadband instruments were prohibitively expensive.

2.3.4 Broadband data versus short-period data

Before portable broadband seismometers became affordable, there was a significant gap in the range of frequencies studied at volcanoes. While deformation techniques, such as those employing tiltmeters, are able to record changes which happen over a period of several minutes, and short period seismology could detect motions above 0.5 Hz, instruments sensitive to the range 1-100 s were not readily available. It was assumed that little, if any, signal of volcanic origin occured within this frequency range. However, broadband studies at Stromboli [*Neuberg et al.,* 1994], Aso [*Kaneshima et al.,* 1994], Mt. Erebus [*Rowe et al.*, 1998] and Kilauea [*Ohminato et al.,* 1998] have shown emphatically that this is not so.

Ground motions in the range 0.01-1 Hz have the potential to elucidate the distribution of pressure sources and the dynamics of magma movement during an eruption. Strainmeters and tiltmeters are usually operated with a sampling rate that is comparable to the repose period of Stromboli, and are therefore inadequate. Short-period seismometers are insensitive to the slow movements of magma or

slow pressure build up prior to eruptions. Consequently only broadband seismology can provide a direct link between observed ground motion and the internal dynamics of the volcano.

Tilt-induced signals

Horizontal components of a seismometer measure the acceleration of the seismometer mass along a direction orthogonal to gravity (assuming that gravity acts vertically). However, if the seismometer is tilted from this horizontal plane, the acceleration of the mass will no longer be just the ground displacement, as there will also be a contribution from gravity. This unwanted contribution is called the 'tilt-induced signal' and can arise from inflation of the volcano or settling of the base on which the seismometer sits. Tilt-induced signals on vertical components are negligible. Short-period seismic phases are relatively immune to tilt-induced signals, which are proportional to the square of the period of the source [e.g. *Aki and Richards*, 1980].

Forbriger and Wielandt [1997] show that in the near-field the tilt-induced signal is proportional to the double time integral of the vertical component of ground motion and demonstrate how to remove it in order to recover the horizontal ground motion. They find that for VLP phases recorded at Stromboli in 1995, the tilt and corrected displacement have an equal amplitude for a period of ~50 s.

2.3.5 SP eruption signals

Short period eruption signals at Stromboli

SP eruption phases (often referred to as 'explosion quakes') have been studied extensively [e.g. *Mariotti et al.*, 1976; *Ntepe and Dorel*, 1990; *Braun and Ripepe*, 1993; *Ripepe et al.,* 1996; *Ereditato and Luongo*, 1997]. They typically show an emergent low-frequency (1-2 Hz) onset followed by a higher-frequency, higher amplitude phase (3-4 Hz) [Fig. 2.6; *Ereditato and Luongo,* 1997].

The low-frequency phase is linearly polarized, whereas the high-frequency phase has a chaotic particle motion [*Ereditato and Luongo*, 1997]. *Neuberg et al.* [1994] found the low-frequency phase to be dominated by surface waves, whereas phase velocities suggest that the high-frequency phase is a ground-coupled air-wave [*Braun and Ripepe*, 1993]. The phase velocity of the first phase has been variously

reported in the range 600-1600 m/s [*Ereditato and Luongo;* 1997*; Braun and Ripepe,* 1993].

Ripepe et al. [1993] identified two types of signals rather than two distinct phases. Type 1 events have a monochromatic 0.8 Hz spectrum, and high seismic energy, whereas type 2 events have a wider band spectrum peaking at 2.1 Hz, and high kinetic energy. It is not possible however to identify at which vent the eruption occured from analysis of the short-period record alone.

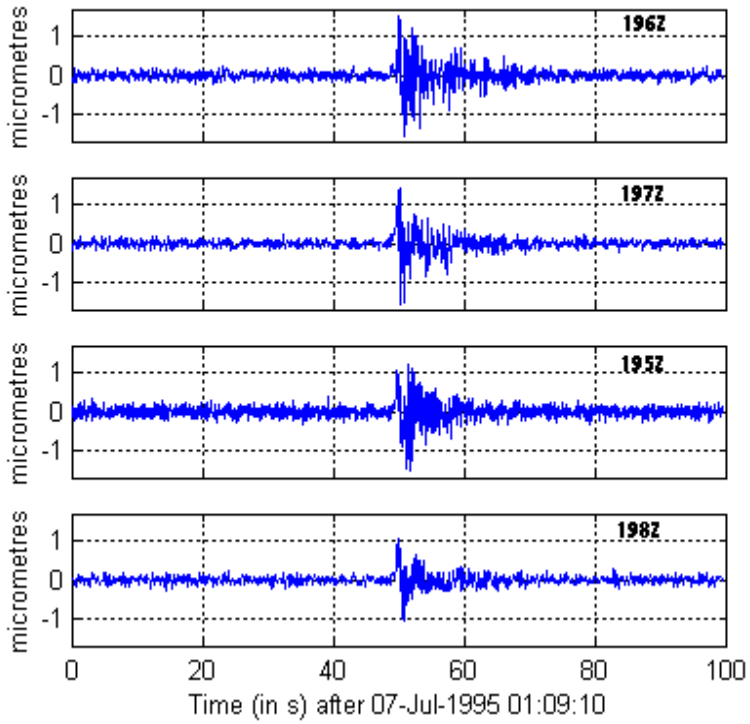

Figure 2.6: Short-period phases corresponding to an eruption at vent 1. Shown (from top) are the vertical components for stations 196, 197, 195 and 198, using the same scale. Interpretation of these seismograms is difficult. Signals like these are often called 'explosion quakes' as they are believed to be caused by a bubble exploding at the air-magma interface. An air-wave can often be identified (but not on this example).

Source location

Travel-time and polarization analyses of these events indicates a shallow seismic source less than 200 m below the vents [*Mariotti et al.*, 1976]. *Braun and Ripepe* [1993] used the variable travel time difference between the direct P wave and the ground-coupled airwave as evidence of changing sound speed in the conduit. Assuming these waves have the same origin, they conclude that the source is 50–150 m below the crater area. Combining this with the delay times leads them to conclude that the sound speed in the conduit is 20–80 m/s, which is certainly possible in a bubbly fluid [*Kieffer*, 1977]. Other studies [*Capaldi et al.,* 1978; *Del Pezzo et al*., 1992] recognised that the data were not sufficient to obtain a reliable estimate of source depth.

There are problems with the methods used:

1. The low-frequency phase has an emergent onset. This suggests that hypocentres determined by travel-time analysis are prone to large errors. Since hypocentres have been determined for very few events, this suggests that there might be very large error bars on this source depth of 200 m.

2. The rectilinearity of the particle motion of these phases is low [*Luckett*, 1997]. This suggests large errors in hypocentres determined by polarization analysis. To compound this, *Neuberg et al*. [1994] found the polarization steepens as lower frequencies are considered, only becoming stable below 0.4 Hz, as higher frequencies are dominated by scattered surface waves. This suggests that the true depth is somewhat deeper than 200 m. This frequency dependence arises because material inhomogeneities need to be at least one-quarter of a wavelength in size to scatter a wave. The interaction with the free surface is particularly strong, and its effects must be removed by applying a surface correction [*Neuberg and Luckett*, 1996; *Neuberg and Pointer*, 1999].

Ripepe et al. [1993] suggested that an alternative estimate of source depth may be obtained from the ratio of observed kinetic to seismic energy, since ejecta from deeper eruptions are less likely to reach the vents. However, a quantitative method for doing this has not been derived.

Seismic source

There is debate over the nature of the source of the low-frequency phase. *Ereditato and Luongo* [1997] believe that seismic waves are produced by the resonance of a shallow magma body, whereas others attribute the source to an explosion at the top of the magma column, generated by rising gas bubbles reaching the surface [e.g. *Braun and Ripepe*, 1993; *Ripepe et al.,* 1996]. Perhaps the main reason that so little progress has been made in this debate is that short period signals are generally very hard to interpret in terms of an underlying source process. This lead *Neuberg and Luckett* [1996] to conclude that short-period signals contain 'nothing that can shed light on the source mechanism...a muddled burst' [e.g. Figs. 2.5 & 2.6].

2.3.6 VLP signals

Broadband recordings reveal significant very-long-period (1-30 s) components to the eruption signals discussed in the previous section. These phases are highly coherent [Fig. 2.8], indicating an isotropic source, in contrast to SP phases. Polarization analysis benefits a great deal when applied only to the VLP part of the seismic signal [*Neuberg and Luckett*, 1994]. Other benefits of broadband recordings are:

(1) the seismic signature alone is sufficient (in 90% of cases) to determine at which vent an eruption occured [Fig. 2.7; *Neuberg et al*., 1994], and,

(2) broadband waveforms are much simpler to interpret [Fig. 2.5].

The variety of VLP phases observed at Stromboli is discussed in the following subsections.

VLP phases corresponding to vent 1 eruptions

The broadband seismic signature of eruptions at vent 1 resembles the letter W [*Neuberg and Luckett*, 1994]. Based on seismic data recorded in 1992, *Luckett* [1997] found this W-shaped signal consists of two distinct VLP phases:

(1) An 'underlying wavelet' with a period of ~16 s, which usually has a trough or peak-trough waveform and,

(2) a 'notch phase', with a period of 2-4 s.

The amplitude of the underlying phase correlates with amount of ejecta. The notch phase precedes the eruption by a variable amount. The first motions of each of these phases suggest a contraction (or implosion). These events vary in amplitude by a factor of 2 or 3, and the relative arrival times of these phases varies too, leading to a range of waveforms. The visible eruption corresponds to the second drop of the W indicating motion towards the crater region.

The P wave speed is approximately 1200 m/s if the eruption and seismicity have the same source. Also if a speed of 340 m/s is assumed for the observed ground-coupled airwave, it may coincide with the onset of the underlying phase. The underlying phase and the notch phase have different source locations.

VLP phases corresponding to vent 2 eruptions

In the 1992 dataset the signature of type 2 events was a weak, wide-stretched trough [*Neuberg and Luckett*, 1997]. This is probably because the ejecta were almost entirely gas. The impedance contrast between rock and gas is very large, leading to poor coupling and a reduced seismic response. Since these phases are difficult to measure, vent 2 eruptions are considered no further.

VLP phases corresponding to vent 3 eruptions

In the 1992 dataset the broadband seismic signature of type 3 events is very similar to the underlying wavelet corresponding to eruptions at vent 1 (suggesting a common source), but shorter in period (~13 s rather than ~16 s). In addition to this V-shaped signal, oscillations are often observed; these have emergent onsets and are sinusoidal with a frequency range of 0.65-0.95 Hz [*Luckett*, 1997].

Analysis shows that the oscillatory phase begins first, and that the underlying wavelet is produced by eruptive flow. The first ejecta are observed at about the same time as the oscillation peaks. About 1 s before this an air wave is generated in the vicinity of the vent. The amplitude of the underlying wavelet correlates with the amount of ejecta.

VLP phases in the 1995 dataset

The VLP signals recorded in 1995 differ slightly from those recorded in 1992. This is partly because they were recorded much closer to the vents, but it is also possible that the source mechanism changed slightly over the intervening period. However, the same general features are observed. Events corresponding to eruptions from vent 1 still show a W-shaped waveform [Fig. 2.7a] and those from vent 3 show a

(small) V-shaped waveform [Fig. 2.7b]. The W-shaped waveform is clearly preceded by inflation of the volcano, probably indicating pressure build-up. The V-shaped waveform is superimposed on a much larger and longer duration inflation-deflation phase. Both of these features are shown far better in the 1995 dataset, probably because the stations are much closer to the source. No detailed study of the 1995 dataset has been performed to date other than the modelling work presented in this thesis.

Incoherent signals at very-long periods (or even longer) could be due to the migration of magma in the feeding system since the modelling performed in Chapters 4 and 5 suggests that magma migration would lead to signals which would have the appearance of incoherent noise. However, because the signals are continuous, it is impossible to test this hypothesis.

Source location of VLP phases

In contrast to the shallow source locations found with short period data, *Luckett* [1997] found evidence for deep sources. On the basis of travel-time and polarization analysis of the VLP signals described above, *Luckett* [1997] finds the following source locations:

(1) underlying phases corresponding to eruptions at vents 1 and 3 have a common origin, 700 m beneath the vents,

(2) the location of the notch phase (vent 1) is approximately 100 m above this,

(3) the oscillatory phase has a source depth of 300 m and coincides with a linear source area of magmatic dykes associated with a previous centre of activity.

The locations of *Luckett* [1997] are much deeper than those found by analysing SP phases. However, *Neuberg et al*. [1994] found the polarization steepens as lower frequencies are considered, only becoming stable below 0.4 Hz, as higher frequencies are dominated by scattered surface waves [*Neuberg et al*., 1994].

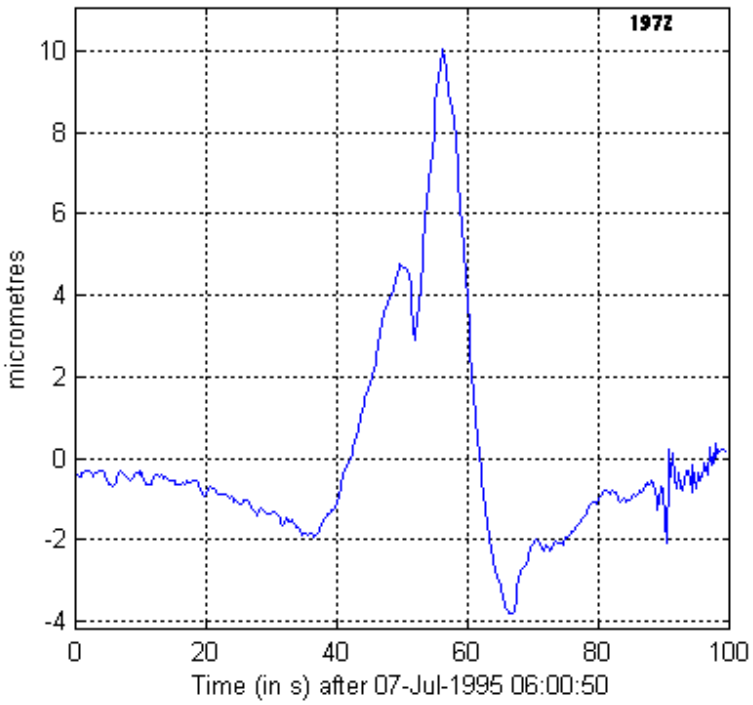

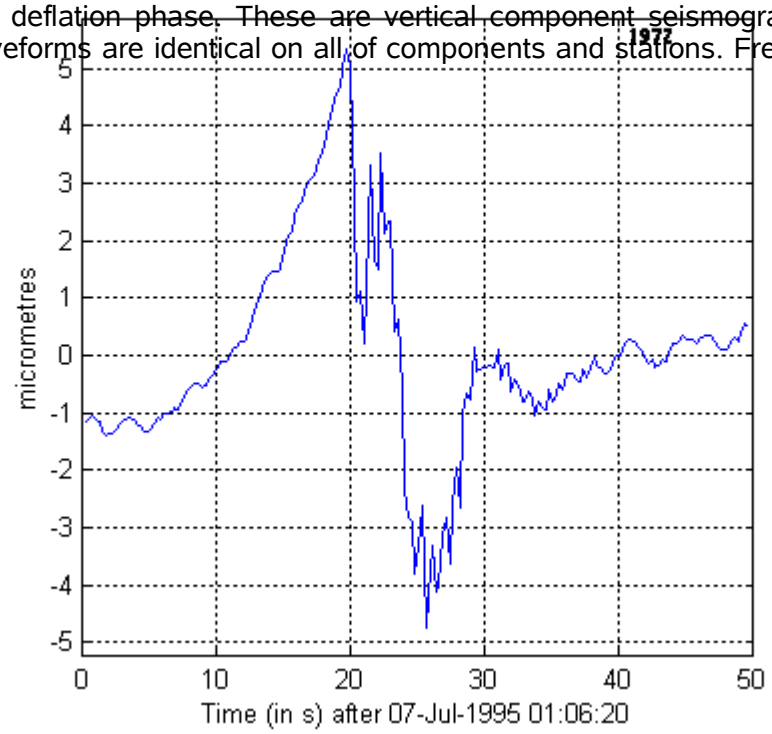

Figure 2.7: Characteristic waveforms corresponding to an eruption at (a) vent 1 and (b) vent 3. Vent 1 signals consist of an inflation phase with increasing slope, followed by a W shaped deflation phase. Vent 3 signals consist of 2 inflation phases separated by a small V shaped signal, then a large deflation phase. These are vertical component seismograms recorded at station 197, but waveforms are identical on all of components and stations. Frequency range is 0.01-7.8 Hz.

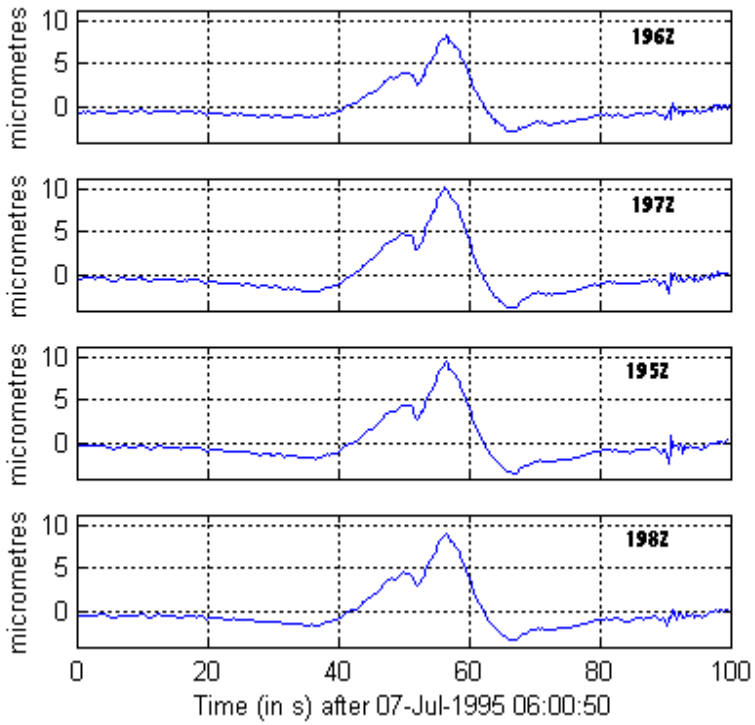

Figure 2.8: Vertical seismograms showing VLP phases corresponding to a vent 1 eruption. These signals are remarkably coherent (demonstrating the azimuthal symmetry of the source), and almost identical in amplitude.

Forbriger and Wielandt [1997] studied broadband data collected at Stromboli in 1995, but they removed the effect of tilt prior to using a Mogi half-space based solution to locate the source of the displacement signal and the tilt signal. They found that these signals share a common source, 135 m below the craters. It seems likely that the same source depth would have been found had they not separated the signals, so the results of *Forbriger and Wielandt* [1997] are at odds with the much deeper source depths indicated by *Luckett* [1997] for the same signal type.

Chouet et al. [1999] used semblance analysis to determine the source location of VLP signals and concluded the source region is located about 300 m north-west of and 300 m below the vents. This study invalidates the assumption made by both *Luckett* [1997] and *Forbriger and Wielandt* [1997] that the source lies directly beneath the vents.

Because the source locations are so important for the modelling attempted in this thesis, some of the 1992 and 1995 data published in *Luckett* [1997] were re-examined to see how robust the source locations of *Luckett* [1997] are. A new travel-time analysis (performed for this thesis) showed:

- Data from the 1992 experiment are consistent with a source directly beneath the crater region, but the residuals are smallest for a source 300 m ENE of the craters.

- Data from the 1995 experiment are inconsistent with a source located beneath the crater region. Residuals are smallest for a source 200 m NW of the craters.

- The source locations found using 1992 and 1995 data (which had different array configurations) are not consistent within 1 standard deviation. This may be because the active source has moved (which seems unlikely) or because the source is not a point source (which was assumed for the inversions) or most likely because the travel-times were not measured with sufficient precision to find a robust solution.

- There is good evidence that the average P wave speed of the mixture of lava and ash layers is approximately 1700 m/s since all inversions converge to a value close to this. This is in agreement with results obtained from seismic refraction profiling [*Roger Clark, University of Leeds*, pers. comm., July 1999] and differential travel times [*Braun and Ripepe*, 1993].

Source depth is poorly constrained in both 1992 and 1995 datasets. A source near sea level follows only if one assumes that the source lies directly beneath the vents [e.g. *Luckett*, 1997]. Unfortunately the depth and horizontal positions are coupled. A much shallower source is also consistent with the data. The particle motion results of *Luckett* suggest either a line source aligned vertically beneath the craters, or a point source close to sea level, although tilt was not corrected for and the surface correction applied was not correct [*Neuberg and Pointer*, 1999]. The conclusion is that there is only weak evidence for the source locations of *Luckett* and that they cannot be relied upon for modelling purposes. It should be added, however, that there is no reason for believing the source locations found by any other study are any more reliable.

Seismic source

The most remarkable thing about the broadband data is that they show that the source region contracts very sharply immediately prior to, or at the onset of, each eruption. These sharp contractions indicate a rapid pressure drop in the source region. A somewhat slower pressure rise occurs before these contractions are observed.

The ash cloud associated with eruptions at vent 1, suggests that a cap rock (or skin of cooled magma) forms in the conduit between eruptions (although the ash maybe primary). Meanwhile vent 3 is thought to remain open between eruptions. This may explain why although an underlying phase is observed for eruptions at both vents, a notch phase is only observed in association with vent 1 eruptions. It seems likely therefore that the pressure drop indicated by the notch phase is related to the failure of a cap rock. *Neuberg and Luckett* [1994] suggest the pressure drop indicated by the underlying phase is due to the Bernoulli effect.

2.3.7 Tremor

Volcanic tremor is a continuous seismic signal, which usually has a peak frequency of around 2 Hz. Tremor is important because high tremor amplitudes generally coincide with high explosivity at Stromboli [*Nappi*, 1976] and at other volcanoes [e.g. *McNutt,* 1994].

It is generally believed that tremor at Stromboli is generated by small continuous bubbles bursting at the top of the magmatic column [*Ripepe et al.,* 1993; *Ripepe,* 1996; *Ripepe et al*., 1996]. *Neuberg and Luckett* [1996] showed that a random sequence of bubbles bursting in a pipe can cause lead to a spectrum resembles tremor. The bursting bubbles may cause the conduit to oscillate at its harmonic frequencies. However harmonic tremor has not been recorded at Stromboli, indicating perhaps that open vents cannot sustain long term resonances. Further evidence for this mechanism is the continuous degassing and flaring observed at vent 3, which suggests bubbles bursting at the top of the magmatic column [*Neuberg et al*., 1994].

Tremor at Stromboli has a frequency content of 1-5 Hz [*Ripepe et al*., 1996] and stable peaks. The same authors suggest that frequency content is related to gas overpressure present in bursting bubbles. The spectral characteristics of volcanic tremor are also similar to those observed for low frequency signals (basically anything below 3 Hz), perhaps indicating a common source [*Ntepe and Dorel*,

1990; *Del Pezzo et al*., 1992; *Ripepe et al*., 1993]. However, *Luckett* [1997] finds that at Stromboli the dominant peaks are site dependent which suggests they cannot be used to deduce anything about the source. *Ripepe et al*. [1996] report that tremor and infrasonic waves also have the same origin, based on energy profiles and spectra.

2.4 Character of the magmatic system

2.4.1 Deep source

Petrological data and velocity anomalies suggest there may be pooling of primary magma at a depth of 10-14 km. This may be where less soluble gases such as carbon dioxide are exsolved, and as magma rises these small bubbles act as seeds for the more abundant, more soluble gases such as sulphur dioxide.

2.4.2 Shallow reservoir

Other than drilling, which is prohibitively expensive, there is no way to obtain direct evidence of the shallow magmatic system. At several volcanoes the position and approximate size of a shallow reservoir has been imaged with either seismic tomography or b-value mapping [*Wiemer and McNutt*, 1997]. However, these techniques require a dense, well-distributed seismic network, which has never been deployed at Stromboli. Swarms of volcanic-tectonic earthquakes are also useful at many volcanoes for determining the position of shallow magma bodies. These events occur in response to changes in the local stress field caused by movements of magma. However, VT events are rarely observed at Stromboli, which suggests that magma conduits remain open.

At Stromboli, lava effuses at a rate of less than 2 kg/s and yet the observed sulphur dioxide flux can only be explained by the degassing of at least 200 kg/s of magma [*Allard* et al., 1994; *Giberti* et al., 1992]. Once magma is degassed it cannot generate further eruptions, so it must be removed from the conduit and accumulate elsewhere.

Allard et al. [1994] propose that degassed magma is removed by the convective overturn of a magma chamber, which acts to homogenise the mix. They remark, however, that convective overturn of a magma chamber would only be an efficient way to remove degassed magma from the conduit if the conduit were less than 400 m long. This indicates a shallow magma chamber, which because of Stromboli's conical form, cannot be more voluminous than a few km^3. Such a volume is insufficient to account for the SO_2 flux assumed roughly constant over 5000 years, so there must be a constant supply of gas-rich magma from below, and a mechanism for the removal of degassed magma from the magma chamber.

Francis et al. [1993] speculate that the degassed magma is ultimately removed because it intrudes voids created by downward and outward extensional faulting. This is consistent with the gravitational instability of the NW flank, marked by the Sciara del Fuoco, which allows fractures along a NE-SW direction, which is the direction along which vents are aligned. The consequent growth of Stromboli over the past 5000 years is estimated at between 5% and 50% [*Giberti et al*., 1992; *Allard et al.,* 1994].

Modelling by *Buckingham and Garces* [1996] indicates that the conduit is bounded by a shallow magma chamber. From the thermal effects of degassing, they also conclude that the two-phase gas-magma mixture originates at a depth no greater than 200 m. This may correspond to the roof of a shallow magma chamber [*Jaupart and Vergniolle*, 1988].

2.4.3 Surface conduit

The vents at Stromboli are almost certainly linked to the same magma source, but at some point they must diverge from each other, perhaps in a dendritic network of pipes and cracks near the surface.

Finite element modelling by *Giberti et al*. [1992], based on the assumption of thermal stability, suggests a conduit radius of 1 m and a conduit length of 100 m. If the conduit widens with depth, the conduit would need to be even shorter. A short conduit suggests a shallow magma reservoir.

It is reasonable to assume that conduits are both cylindrical and smooth, at least in the uppermost parts, because of the stability of the activity at Stromboli over the past several thousand years [*Kieffer and Sturtevant*, 1984]. If early eruptions at Stromboli began with the propagation of narrow fissures from magma reservoirs to

the surface, then over time, rising magma would tend to erode the fissure wall, and slow rising magma at the margins of a fissure would cool and solidify. The combined effect would a more circular conduit.

2.4.4 Summary

There are few data about the magmatic system at Stromboli, or indeed at any other volcano. However, the literature that does exist suggests the following, general outline. Primary magma may gather in a magma reservoir at the base of the crust. This replenishes a very shallow magma reservoir the top of which may be as little as 100 below the active vents, implying a short conduit. Thermodynamic arguments suggest this conduit is relatively narrow, a radius of 1 m being a good order of magnitude approximation: this is about the radius of the active vents. Longevity of the activity at Stromboli suggests this conduit is approximately circular in cross-section.

Fortunately for modelling purposes, a more detailed understanding of the magmatic system is not really necessary, since it would be difficult to model these details anyway. Therefore during the remainder of this thesis a shallow magma reservoir will be assumed along with a single, cylindrical conduit.

2.5 Modelling parameters

Before any modelling can be attempted, model parameters must be determined. The physical variables of interest are conduit or chamber radius, conduit length, magma rise speed, overpressure, pressure gradient, density in the fluid and solid, P wave speed and S wave speed in the fluid and solid, fluid viscosity and peak mass flux rate.

- P wave speed in the rock is well constrained. Inversions of travel-times corresponding to VLP phases at Stromboli suggest α_s=1700 $\pm$ 200 m/s, a result supported by a seismic refraction experiment [*Roger Clark, University of Leeds*, pers. comm., July 1999] and *Braun and Ripepe* [1993]. Surprisingly, *Eredidato and Luongo* [1997] found a P wave speed of 600-800 m/s. In this thesis a value of 1700 m/s is used.

- P wave speed in a magma/gas mix can be very low if there is significant presence of bubbles, as the mix becomes highly compressible, yet has a density comparable to that of rock [*Kieffer*, 1977]. Based on seismic waves and air waves having the same origin *Braun and Ripepe* [1993] compute α_f=50-70 m/s in the upper part of the conduit. For modelling it is that average P wave speed in the conduit which matters more, and this increases with depth as there are less bubbles (higher density, less compressibility). *Vergniolle et al*. [1996] use a value for the P wave speed in magma to be > 2500 m/s for Stromboli, which is larger even than estimates of P wave speed in rock, and would imply a very leaky source. It seems there is no consensus, but fortunately this parameter is not critical in a narrow conduit – all it does is affect the arrival time very slightly and lead to slightly different amplitudes because of the impedance contrast at the conduit wall. A value of 500 m/s is used in the modelling that follows.

- *Vergniolle et al.,* [1996] state that viscosity (η) must be no more than 1000 Pa s, and chose a value of 300 Pa s, for modelling of sound waves generated at the magma/air interface. *Blackburn et al*. [1976] use a value of η=100 Pa s, but they are more interested in an average value as the magma rises from depth. Viscosity is likely to be somewhat lower with increasing depth because an increasing amount of volatiles are dissolved and magma temperature increases slightly. It seems reasonable that as over the final few hundred metres of ascent the viscosity may vary from 100-1000 Pa s.

- *Vergniolle et al*. [1996] model the conduit at Stromboli as a cylinder of radius r=1 m (which is the vent radius observed at the surface) with a length of several hundred metres, and a bubble rise speed of around 1.6 m/s. They compute a Reynolds number of ~80 which indicates that viscous forces dominate. There are no data for the radius of the conduit at depth, but *Wilson* [Lancaster University, pers. comm., September 1997] suggested that conduits widen with depth and become more rectangular in cross-section. *Buckingham and Garces* [1996] modelled the sound field using r=16 m, which far exceeds other estimates, and a conduit length l=100 m, which is very short. In addition they find a source depth of 83 m and a source pressure of 1 GPa. Thermodynamic constraints [Chapter 2] suggest the conduit is no more than 200 m long and 1 m in radius, but this implies a small shallow magma chamber which could not support continuous activity over several millenia. It seems likely that the conduit may widen with depth, from 1 to several metres in radius, and is between 200 m

and several hundred metres long. In this thesis a maximum conduit length of 700 m long is assumed, since this is the geometry most consistent with the results of *Luckett* [1997], which are themselves probably the most reliable measurement of seismic source depth.

- *Vergniolle et al*. [1996] estimate overpressures within bubbles of 1 m radius at Stromboli to be in the range of 0.1 MPa to 0.6 MPa. The maximum overpressure that can develop in a magma chamber are probably of the order of 10 or 20 MPa [*Tait et al.,* 1989].

- One very useful parameter is mass flux, i.e. the mass of ejecta leaving the vent in one second. *Chouet et al*. [1974] report a peak volume flux of gas of ~ 1000 m^3/s and a gas density of 200 kg/m^3, which gives a mass flux of 200 kg/s. Gas exits the vents at 50-100 m/s [*Blackburn et al,* 1976; *Chouet et al.*, 1974, *Ripepe et al*., 1993]. Solid or liquid ejecta are ejected at much lower speeds and in rare cases may account for almost half of the ejected mass. The mass of ejecta issued in a single explosion is typically less than 1000 kg. Again this indicates a mass flux of <1000 kg/s.

- Rock density is ~ 2700 kg/m^3. Fluid density depends on the volume fraction of bubbles. If there are no bubbles, fluid density is almost the same as rock density. If the volume fraction of bubbles is 0.5, the fluid density will be around half of rock density.

2.6 Seismic sources and volcanic processes

2.6.1 Distinction between seismic sources and volcanic processes

Volcano seismologists are particularly interested in recording seismic phases which are precursors to eruptions. To deduce what those precursors mean, they must be related to the underlying physical processes. However, processes which lead to the generation of large seismic waves are not necessarily the same processes that lead to eruptions. For example, fragmentation is perhaps the most fundamental process that occurs prior to a Plinian eruption, but a seismic phase corresponding

to fragmentation has never been identified. There is a need to investigate which volcanic processes have the potential to generate large seismic signals. The first step is to investigate Strombolian activity and look at some of the processes involved.

2.6.2 Strombolian activity

The most plausible explanation of the Strombolian explosions is that they represent bursting of large bubbles at the surface of the magma. The least soluble gases exsolve at great depth, nucleating bubbles which act as seeds for the diffusion of more soluble (and more abundant) gases at shallow depths. These bubbles grow through a combination of decompression and exsolution, and accumulate an overpressure because viscous forces prevent them from expanding rapidly enough to remain in equilibrium with the surrounding magma. These viscous forces and hence the overpressure increase as the bubble rises, since the magma is increasingly more viscous due to having lost much of its water content.

The decompression of the gas from the bursting bubbles at the magma surface results initially in high gas velocities, rapidly decelerating as the solid/gas dispersion interacts with the atmosphere. The finer grained particles are transported to much greater heights by convection [*Blackburn et al*, 1976].

2.6.3 The transition from strombolian to hawaiian activity

One of the mysteries of Stromboli is that the style of activity at each vent can be quite different, even though they are almost certainly fed by the same magma source. Sometimes the style of activity at an individual vent changes over time too. How can these observations be explained?

Bubble coalescence appears to be the key to the transition from hawaiian to strombolian activity. However it is not clear whether it is increasing [*Jaupart and Vergniolle*, 1988] or decreasing [*Parfitt and Wilson*, 1995] bubble coalescence that leads to the transition from strombolian to hawaiian activity. It is agreed that strombolian activity is the result of gas slugs bursting at the surface, whereas Hawaiian fire fountains can be attributed to annular flow. A third flow regime is bubbly flow which leads to passive effusion; this is observed between eruptions at vent 3 of Stromboli.

Laboratory experiments by *Jaupart and Vergniolle* [1988] suggest that large bubbles are formed by coalescence at the roof of a magma chamber. Within the chamber, small bubbles (<1 cm) rise and accumulate at the roof in a foam layer whose thickness increases. As foam accumulates at the roof buoyancy acts to flatten the bubbles at the roof. As the foam thickens, bubbles are flattened further, until surface tension can no longer sustain this force and the bubbles burst and coalesce, generating gas pockets whose size depends on liquid viscosity and surface tension.

At high viscosity, many gas slugs are produced, which flow into the conduit and burst out intermittently at the vent expelling liquid fragments of the bubble wall upon bursting. Large bubbles burst explosively when they reach the surface because of the substantial pressure gradient between internal bubble pressure and the medium above the bubble [*Sparks*, 1978].

At lower viscosity a single large gas pocket is formed, which flows into the conduit, causing the magma in the conduit to rise. As the gas pocket nears the surface, a fire fountain is produced as the liquid films that wet the conduit walls are ejected. Then a cycle of gas-piston events occurs, causing rise and fall of magma level (but overall rise) until the next fire fountain occurs.

This transition from strombolian to hawaiian activity can also be induced by increasing the gas content of the magma, since this leads to more bubbles in the magma chamber, and therefore an increased tendency for the foam to collapse into a large pocket of gas.

Small bubbles are continually entering the conduit and reaching the surface leading to the continuous activity observed between eruptions.

In the model of *Parfitt and Wilson* [1995] bubble coalescence occurs within the conduit. For low magma rise speeds, gas bubbles are rising in an almost static magma column. The gas becomes concentrated at rather shallow depths, coalescing into large bubbles or slugs. When these burst at the surface, the excess pressure which has formed in the bubble due to viscous resistance is explosively released, giving rise to a strombolian blast. The slow rising magma becomes gas-poor and never becomes sufficiently bubbly to fragment.

If the magma is ascending rapidly, bubbles are transported with the magma, and the chance of coalescence is small. Existing bubbles increase in size as they rise due to a combination of decompression and volatile migration from the magma.

New bubbles nucleate all the time and the magma becomes more and more supersaturated as the pressure decreases. The flow becomes more and more bubbly as it ascends until it fragments (at a relatively deep level). The gas then rapidly expands and the mixture acclerates up the conduit due to this expansion and the virtual elimination of friction with the conduit wall. This leads to the steady discharge of lava clots and gas, forming a lava fountain.

According to this model, the transition from negligible bubble coalescence and lava fountaining to dominant coalescence and strombolian activity occurs at a rise speed of ~0.1 m/s. It is magma rise speed at depth, rather than gas content, that is the most critical factor. Viscosity has little effect. However, for any given magma rise speed, a reduction in gas content results in a reduced amount of coalescence, and so the eruptive style changes from strombolian to hawaiian. In the model of *Jaupart* and *Vergniolle* [1988] it is an increase in the gas content and an increase in the degree of coalescence that leads to this transition!

In both models there is a spectrum of eruptive styles from effusive activity, through strombolian blasts, to fire fountains, which correspond to flow regimes from bubbly flow, through slug flow to annular flow.

2.6.4 Seismic sources

In order to quantify whether a particular volcanic process is a significant seismic source, it is necessary to consider the size of the pressure changes it leads to. The pressure changes associated with several volcanic processes will now be considered:

Magma rise

At great depth below Stromboli there must be an almost constant supply of slowly rising magma, but it seems very unlikely that this motion could generate detectable seismic energy.

At shallow depths, eruptive flow may correspond to magma rise speeds of around 1 m/s. The corresponding pressure changes in the conduit might lead to a signal large enough in amplitude and short enough in period to be identified in broadband seismic records.

Bubble rise

It is not clear whether large bubbles or slugs rising in a conduit could generate a detectable amount of seismic energy. Slugs or large gas bubbles may have an overpressure of several MPa relative to the magma they are rising through [*Vergniolle and Brandeis*, 1996], but the question is whether the pressure in the magma increases significantly as an overpressurised bubble rises through it. Perhaps a separate seismic signature could be identified for bubbly flow, slug flow and annular flow?

Advective overpressure

Related to bubble rise is advective overpressure [e.g. *Sahagian and Proussevitch*, 1992]. In a sealed conduit with a rigid wall and for a bubble which does not have diffusion acting through its walls, the pressure in the conduit increases by an amount ρgh if h is the vertical distance that the that bubble rises (ρ is magma density, g is gravitational acceleration).

Bubble coalescence

Jaupart and Vergniolle [1988] attribute the formation of large bubbles to the collapse of a foam at the roof of a magma chamber. When this foam collapses *Vergniolle and Brandeis* [1996] suggest that it releases a pressure equal to the surface tension of all the bursting bubbles. If true, this pressure drop needs to be quantified.

Bubble or slug burst at the free surface

When large bubbles or gas slugs reach the surface they are highly unstable and oscillate in several modes before bursting explosively. The overpressure in these bubbles results because viscous resistance prevents them from growing fast enough to remain in equilibrium with the surrounding fluid. These oscillations generate air waves which have been studied by numerous authors [e.g. *Vergniolle and Brandeis*, 1994; 1996; *Buckingham and Garces*, 1996]. It is possible that these oscillations and the explosive bubble burst in particular generate detectable seismic waves also. (These vibrations and bursts may also initiate conduit resonance, which is recorded as volcanic tremor). According to *Vergniolle and Brandeis* [1996] the excess pressure within the slug/gas pocket is of the order of the lithostatic pressure at the base of the conduit, which is approximately 10 MPa for a 400-m-long conduit.

Explosive degassing

This can occur from the ascent of magma. The magma contains volatiles which are dissolved at great depth, principally carbon dioxide and water. As the mixture ascends, the pressure diminishes as does the solubility in the magma of these volatiles. When the solubility becomes less than the concentration of volatiles, magma and gas separate to form two distinct phases. If magma rises more quickly than phases can separate, the difference between solubility and concentration increases, resulting in explosive degassing.

Fragmentation

Fragmentation corresponds to the bursting of bubbles, which release excess pressure. Perhaps then fragmentation is characterized by seismic displacement towards the fragmentation zone? For forecasting purposes, it is not particularly useful to identify such a seismic phase because the eruption would follow within seconds.

Rupture

A conduit can become sealed when the magma at its margins cools and solidifies, forming a cap rock at the top of the conduit. At some time later, a new influx of magma may enter the conduit, driving up the pressure, and perhaps partially re-melting the cap. At some point the rising pressure in the conduit may overcome the (decreasing) yield strength of the cap, and explosively release the excess pressure. This pressure drop has the potential to generate large amplitude seismic waves.

The pressure in the conduit does not drop instantaneously to ambient, but rather drops in a series of steps. A rarefaction wave propagates downward, accelerating and expanding the fluid in the upward direction. The rarefaction moves downward with the speed of sound of the undisturbed reservoir fluid. When the rarefaction wave reaches the bottom of the reservoir, it reflects from the rigid wall as another rarefaction, and traverses again the full length of the conduit. In the interval between the passage of the first and second waves all quantities are constant. During this and similar intervals the measured pressure histories show plateaus between the passage of rarefactions. It is through this series of rarefactions that the pressure drops, stepwise, to ambient [*Kieffer and Sturtevant*, 1984].

2.7 Summary

For several thousand years the activity at Stromboli has probably changed very little. In 1992 and 1995 there were three active vents, and around 10 eruptions per hour. The longevity of this activity, together with thermal and degassing budgets, implies:

- narrow cylindrical conduits,
- a small, shallow magma chamber, the top of which is probably less than 400 m beneath the vents,
- continuous supply of new magma, and
- removal of old magma via endogenous growth.

Each vent has its own eruptive style (though this sometimes changes) and characteristic VLP seismic signature. These VLP phases are an order of magnitude larger than the corresponding short-period events, have much simpler waveforms, and are more robust for modelling purposes. Three VLP phases have been identified: an underlying phase corresponding to eruptions at vent 1 (16 s) and at vent 3 (13 s) and a notch phase corresponding to vent 1 eruptions (2-4 s). A deformation phase (~30-60 s) is also observed for both vent 3 eruptions in the 1995 dataset, though it is often obscured by noise.

Short-period data suggest a shallow seismic source, perhaps no more than 200 m below the crater area, but the short-period wavefield is contaminated by secondary surface waves, suggesting the primary source is deeper. Polarization analysis and travel-time analysis of VLP phases [*Luckett*, 1997] suggests a source located at a depth of 600-700 m, but only if the source position is 'fixed' beneath the vents. Data recorded in 1995 are not consistent with this location. *Forbriger and Wieldandt* [1997] place the source much shallower, 135 m beneath the vents, using a Mogi source which is not appropriate for modelling dynamic displacement. All these estimates are flawed in some way.

Chouet et al. [1999] determined the source of VLP phases to be 300 m below and north-west of the vents using semblance analysis. This appears to be the most reliable result. Polarization analysis and travel-time analysis of VLP phases [*Luckett*, 1997] suggests a source located at a depth of 600-700 m, and using a

Mogi source *Forbriger and Wieldandt* [1997] put the source 135 m beneath the vents, but both of these studies assume that the source lays beneath the vents. Determinations of the short-period source location are misleading since the short-period wavefield is dominated by secondary surface waves.

Strombolian blasts are attributed to the bursting of large, overpressurised bubbles at the surface. However, there is a continuous spectrum of eruptive styles at Stromboli, and it can sometimes resemble Hawaiian or Vulcanian activity. The eruptive style at different vents can be quite different at times, even though they are undoubtedly fed by the same source of magma. Changes also occur in the style of activity at one vent over a period of time. *Jaupart and Vergniolle* [1988] and *Parfitt and Wilson* [1995] have demonstrated that the links between different eruptive styles are quite subtle, and depend primarily on the degree of bubble coalescence.

There is no fundamental reason why processes which ultimately lead to an eruption (e.g. bubble burst) should generate seismic waves. It is therefore important to think about which processes are potential seismic sources. These include rising magma, rising and bursting bubbles, fragmentation, foam collapse and rupture of a sealed conduit. In Chapter 4 some of these processes will be modelled.